Author(s): Ahonen, Salla A.; Vuorio, Kristiina M.; Jones, Roger I.; Hämäläinen, Heikki; Rantamo, Krista; Tiirola, Marja; Vähätalo, Anssi V.

Title: Assessing and predicting the influence of chromophoric dissolved organic matter on light absorption by phytoplankton in boreal lakes

Year: 2024

Version: Published version

Please cite the original version:

Ahonen, S. A., Vuorio, K. M., Jones, R. I., Hämäläinen, H., Rantamo, K., Tiirola, M., & Vähätalo, A. V. (2024). Assessing and predicting the influence of chromophoric dissolved organic matter on light absorption by phytoplankton in boreal lakes. Limnology and Oceanography, Early View. https://doi.org/10.1002/lno.12495

LIMNOLOGY and OCEANOGRAPHY

ASLO

Limnol. Oceanogr. 9999, 2024, 1–12

doi: 10.1002/lno.12495

Assessing and predicting the influence of chromophoric dissolved organic matter on light absorption by phytoplankton in boreal lakes

Salla A. Ahonen [1*] **Kristiina M. Vuorio** [2] **Roger I. Jones** [1] **Heikki Hämäläinen** [1] **Krista Rantamo** [1] **Marja Tiirola** [1] **Anssi V. Vähätalo** [1]

[1]Department of Biological and Environmental Science, University of Jyväskylä, Jyväskylä, Finland
[2]Finnish Environment Institute, Helsinki, Finland

Abstract

Many boreal lakes are colored brown due to strong light absorption by chromophoric dissolved organic matter (CDOM), which reduces light penetration into the water column. However, the influence of CDOM on the fraction of photosynthetically utilizable radiation (PUR) absorbed by phytoplankton from the photosynthetically active radiation (PAR) entering the lake (i.e., PUR/PAR) remains largely unknown. Here, we (1) quantified PUR/PAR values and examined the major water quality parameters determining PUR/PAR from 128 sampled boreal lakes, (2) predicted PUR/PAR values for 2250 reference boreal lakes, and (3) estimated the response of PUR/PAR to typical browning trends reported in earlier studies. The PUR/PAR values ranged from 0.4% to 17% in the sampled lakes, and a logarithmic model including CDOM and chlorophyll *a* (Chl *a*) concentration was the most parsimonious for predicting PUR/PAR values. Applying the model to the reference lakes, PUR/PAR values ranged from 0.5% to 20% (median 3%). In the model, an increase in CDOM content decreases the PUR/PAR value, but a concurrent increase in Chl *a* concentration with the CDOM partly compensates the negative effect of CDOM on the PUR/PAR values. Assuming that browning increases both CDOM and Chl *a* contents, as found for our reference lakes, our model suggests that the decrease in light absorption by phytoplankton in response to a typical degree of browning is only moderate. The moderate response of the PUR/PAR to browning may be explained by photoacclimation of phytoplankton to lowered light availability, and/or an increased loading of nutrients to lakes both leading to higher Chl *a* concentration.

Chromophoric dissolved organic matter (CDOM) has optical properties which, along with those of suspended particulate matter and H_2O, determine the availability of light in aquatic environment (Kirk 2011). In many lakes, CDOM is the most important light-absorbing component, which stains water brown and reduces the depth of the euphotic zone (Jones and Arvola 1984; Kallio 2006; Thrane et al. 2014; Ylöstalo et al. 2014). When CDOM reduces the euphotic depth, it restricts the distribution of benthic primary producers and their photosynthesis to shallow water (Chambers and Kalff 1985; Daniels et al. 2015). In lakes with high CDOM, reduced availability of light for benthic producers can decrease the overall primary as well as secondary production of the entire lake ecosystem (Karlsson et al. 2009; Ask et al. 2012). The impact of CDOM on the light availability for phytoplankton, which is largely responsible for pelagic photosynthesis, is less known but often considered negative (e.g., Karlsson et al. 2009; Thrane et al. 2014). Naumann (1929) categorized brown-colored lakes as dystrophic and concluded that production of phytoplankton is generally low in dystrophic lakes. Phytoplankton cannot capture those photons absorbed by CDOM, but turbulent mixing even in high-CDOM lakes transports phytoplankton to and from the well-lit surface layer and hence alleviates potential light limitation (e.g., Reynolds et al. 1990).

Lakes with high CDOM content have typically elevated concentrations of dissolved organic and inorganic nutrients, which are imported to lake water along with other allochthonous matter from the terrestrial catchment (Thrane et al. 2014; Hamdan et al. 2021; Lepistö et al. 2021). The CDOM content in lakes varies naturally by two orders of magnitude (e.g., between 0.6 and 74 m^{-1} in 3549 Finnish lakes) when quantified as the

*Correspondence: salla.a.ahonen@jyu.fi

Additional Supporting Information may be found in the online version of this article.

Author contribution statement: S.A.A., A.V.V., R.I.J., and K.M.V. conceptualized and designed the study. K.M.V. contributed to the collection of the samples. K.M.V., S.A.A., and K.R. contributed to the laboratory analyses of the samples. S.A.A. and A.V.V. planned the data analyses. S.A.A. performed the data analyses. S.A.A. prepared the initial draft and created the graphs. All authors contributed to the writing and revision of the manuscript.

absorption coefficient at the wavelength of 400 nm ($a_{CDOM}(400)$; Kallio 2006). In CDOM-rich lakes, the elevated concentration of nutrients has the potential to increase Chl *a* concentration and phytoplankton biomass, which can help to compensate for the reduced availability of light caused by CDOM (Bergström and Karlsson 2019; Sherbo et al. 2023). Due to this compensatory effect, the extent to which phytoplankton actually experiences reduced light availability in lakes with different CDOM contents remains poorly known.

In recent decades, the CDOM content of surface waters across the boreal zone has increased and made water darker and browner (Evans et al. 2006; Monteith et al. 2007; Kritzberg and Ekström 2012; de Wit et al. 2016). This browning is caused by increased inputs of dissolved organic and inorganic (iron) chromophores (i.e., CDOM) from the terrestrial catchments to surface waters (Xiao et al. 2013; Škerlep et al. 2020). Along with an increased loading of CDOM, browning is often monitored as an increase in dissolved (DOC) or total organic carbon (TOC) and water color (e.g., Tranvik 1990; Thrane et al. 2014; Ylöstalo et al. 2014), while the chromophoric content of DOC/TOC is variable (e.g., Siegel et al. 2002). In the past three decades, the increase in water color value or concentrations of DOC or TOC (i.e., browning) in lakes has been variable (from 8% to over 100%) but typically about 25% (Williamson et al. 2015; Räike et al. 2016; Kritzberg 2017; Lepistö et al. 2021). The increased inputs of allochthonous matter seen as browning are caused by several factors, such as (1) the recovery from anthropogenic acidification (Evans et al. 2006; Monteith et al. 2007; Strock et al. 2014), (2) climate change associated increases in air temperature and precipitation (de Wit et al. 2016; Lenard and Ejankowski 2017), and (3) intensifying land use and forestry practices (Kritzberg 2017; Škerlep et al. 2020; Finér et al. 2021; Nieminen et al. 2021). While the browning increases water color and can reduce light availability, the increased input of allochthonous matter also provides nutrients, which can promote phytoplankton biomass and thus help to compensate for the light limitation (Corman et al. 2018). As brown lakes are projected to become more common in the future (Yang et al. 2022), it will be useful to understand the effect of browning on the light availability to phytoplankton.

Light availability to phytoplankton can be evaluated from water samples by measuring the spectral absorption coefficient of phytoplankton pigments ($a_{phyto}(\lambda)$) over the range of photosynthetically available radiation (PAR) and comparing it to the corresponding values of non-algal particles ($a_{NAP}(\lambda)$), H_2O ($aH_2O(\lambda)$), and CDOM ($a_{CDOM}(\lambda)$) or the sum of all components ($a_{tot}(\lambda)$). The contribution of phytoplankton to the total absorption of PAR (a_{phyto}/a_{tot}) has been reported to vary from 12% to 39% in the Sargasso Sea (Smith et al. 1989) and 5–32% in Greenland fjords (Murray et al. 2015) to 2–28% in Scandinavian lakes (Thrane et al. 2014) and 3–10% in a Canadian reservoir (Watanabe et al. 2015). For the same sites, the fraction of PAR absorbed by CDOM was 0–13%, 6–18%, 37–76%, and 32–55%, respectively. The lower contributions of phytoplankton to light absorption in freshwater systems compared to marine systems suggest that the higher content of CDOM in lakes than in seas can reduce light availability to phytoplankton (Kirk 2011).

Another way to evaluate the light availability involves the calculation of photosynthetically usable radiation (PUR_z; Morel 1978). PUR_z refers to the absorption of photons within PAR by phytoplankton and accounts for the spectral variability of both solar radiation and $a_{phyto}(\lambda)$ (Morel 1978). Morel (1978) introduced a term PUR_z for a specific depth *z* in the ocean, where the distribution of phytoplankton varies with depth and often includes a maximum below the mixed layer owing to high transparency of oceanic water (e.g., $a_{CDOM}(400)$ often $< 0.03\ m^{-1}$). For the boreal lakes examined in this study, we approximated PUR over the entire water column. Our approximation of PUR assumes that PAR is absorbed within the epilimnion, where phytoplankton is homogenously mixed among the other absorbing components as shown for one of our study lakes (Ahonen et al. 2023). When PUR is divided by the PAR entering to the lake, the unitless ratio PUR/PAR quantifies the light availability as a fraction of PAR absorbed by phytoplankton. Our PUR/PAR ratio in lakes is also comparable to the fraction of absorbed PAR by the photosynthesizing tissue of the canopy in the forest next to lakes. For example, in needle-leaf forests characteristic of boreal catchments, the fraction of absorbed PAR is 40–80% and hence higher than in aquatic environments, where non-algal particles, H_2O and CDOM absorb a major fraction of PAR (Majasalmi et al. 2014; Xiao et al. 2015).

In this study, we examined the fraction of PAR absorbed by phytoplankton (PUR/PAR values) in boreal lakes along a gradient of CDOM. We hypothesized that in lakes with increasing CDOM, both decreased light availability due to increased CDOM and the compensation by increased nutrient availability would act on the PUR/PAR values. We sampled 128 boreal lakes along a CDOM gradient and quantified their PUR/PAR values. Competing models were applied to predict the PUR/PAR values with commonly measured water quality parameters in the sampled lakes. The most parsimonious model was used to estimate PUR/PAR values in 2250 reference lakes based on their water quality, focusing on typical boreal lakes, i.e., on 90% of the lakes from 5th to 95th percentile along the CDOM gradient. Finally, using the most parsimonious model, we estimated how browning changes PUR/PAR values in scenarios following possible browning trends (i.e., increase in CDOM content) reported in earlier studies (e.g., Williamson et al. 2015; Räike et al. 2016; Kritzberg 2017; Lepistö et al. 2021). Since PUR/PAR values are relatively time-consuming to determine directly, our models provide a convenient tool to estimate the PUR/PAR values for lakes using widely available water quality parameters.

Materials and methods

Study lakes and sampling

Our study used two lake datasets. The first consists of 128 mostly boreal and a few subarctic dimictic lakes in

Finland (Fig. 1) that were sampled for optical properties and water quality (hereafter referred to as sampled lakes). The lakes were sampled in 2014–2018 during the summer stratification period (May–August), when a significant part of the primary production in boreal dimictic lakes occurs. The sampling period excludes the period of spring turnover when the availability of nutrients can be high, and DOM is less important as a source of nutrients. Later in the summer, when inorganic nutrients have been consumed from the epilimnion, the organic nutrients associated to DOM (and CDOM) may become more important. Water samples were taken with a 30 or 50 cm long water sampler (Limnos Ltd, Finland) as a composite sample from the homogenous surface mixed layer into 1 L high density polyethylene bottles.

The second dataset consists of 2250 regularly monitored Finnish boreal dimictic lakes and data were retrieved from the open access Hertta database portal (Open data service) maintained by the Finnish Environment Institute (https://www.syke.fi/en-US/Open_information). These lakes were used as a reference dataset of boreal lakes (hereafter referred to as reference lakes). 28% of the sampled lakes are included in the reference lake dataset. The data for the reference lakes were restricted to the same season (May–August) as for the sampled lakes and a mean value of each parameter was determined from the data reported between 2010 and 2022. The Hertta database was also the source for lake morphometry characteristics for both the sampled and reference lakes. The parameters gathered for the reference lakes included lake area and volume, mean and maximum depths, concentrations of total phosphorus (tot-P, μg L^{-1}), total nitrogen (tot-N, μg L^{-1}), and chlorophyll *a* (Chl *a*, μg L^{-1}), and water color value (mg Pt L^{-1}). DOC concentrations for the reference lakes were converted from color values with an equation DOC = 0.0872color + 3.55 by Kortelainen (1993).

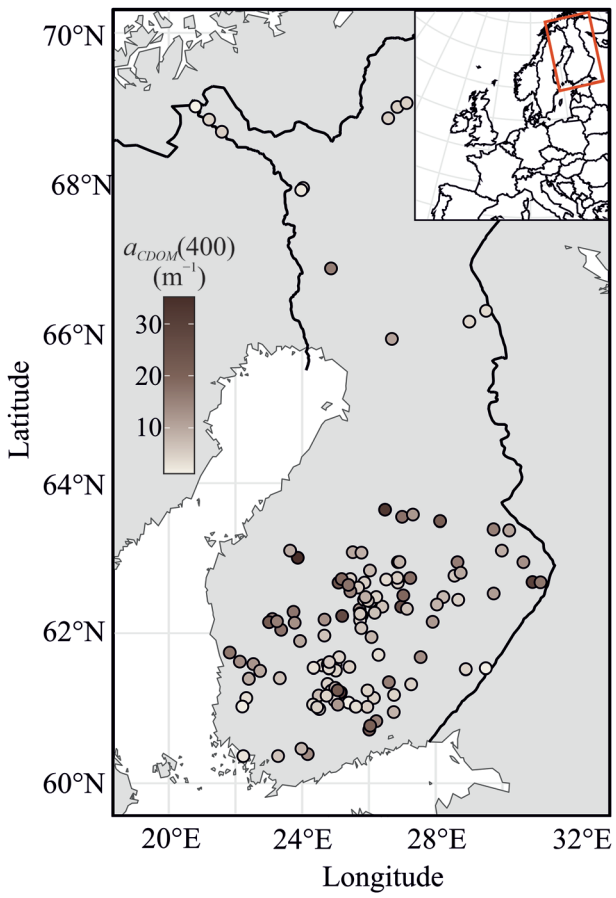

Fig. 1. A map showing the location of the 128 sampled lakes. The color scale indicates the value of $a_{CDOM}(400)$.

Water chemistry measurements

Samples for tot-P and tot-N were frozen (−20°C) and analyzed according to methods in standards ISO/DIS 15681–2 (2005) and SFS-EN ISO 11905-1 (1997) and measured with Gallery™ Plus Automated Photometric Analyzer (Thermo Fisher Scientific, USA). Samples for DOC (mg L^{-1}) were filtered through a polyethylene sulfone syringe filter (Sarstedt, nominal pore size 0.20 μm), stored in acid washed and precombusted glass vials at + 4°C and in the dark. DOC concentration was measured according to high-temperature catalytic oxidation method with a total organic carbon analyzer (TOC-L, Shimadzu, Japan) calibrated with standard solutions of potassium hydrogen phthalate. Chl *a* samples were filtered onto glass fiber filters (Whatman GF/C nominal pore size 1.2 μm, diameter 47 mm) and the concentration (μg L^{-1}) was spectrophotometrically measured with a Shimadzu UV-1800 spectrophotometer (Shimadzu, Kyoto, Japan) after ethanol extraction at 75°C for 5 min (SFS-ISO 10260 1992). Water color (mg Pt L^{-1}) was estimated using an optical comparator (Hellige, Germany) for comparison with hexachloroplatinate reference disks (SFS-EN ISO 7887 2011). In those cases where the lake was sampled more than once, an average value was calculated for each water quality and optical property parameter. For ∼ 10% of the sampled lakes from which tot-P, tot-N, Chl *a*, and water color were not measured, the values were retrieved from the Hertta database as average values from the data collected in May–August between 2010 and 2022.

Absorption measurements

The water samples for optical properties were filtered through glass fiber filters (Whatman GF/F, nominal pore size 0.7 μm, diameter 25 mm). The filtrate was stored in a 50 mL centrifuge tube at + 4°C and in the dark prior to determination of the spectral absorption coefficient of CDOM ($a_{CDOM}(\lambda)$), which was made within 2 weeks of sampling. The values of $a_{CDOM}(\lambda)$ (m^{-1}) were calculated as:

$$a_{CDOM}(\lambda) = \ln(10)\frac{A_{CDOM}(\lambda)}{L} \quad (1)$$

where L is the optical length of the cuvette (0.01 or 0.05 m), $A_{CDOM}(\lambda)$ is the absorbance of lake water at wavelength λ (nm) corrected with a blank (Ultrapure water from Ultra Clear

UV UF TM system; Evoqua Water Technologies) and measured with a Shimadzu UV-1800 or PerkinElmer Lambda™ 650 UV/Vis spectrophotometer. The absorption coefficient of CDOM at wavelength of 400 nm ($a_{CDOM}(400)$) was selected to quantify the CDOM content of lake water, as has been done in previous studies (e.g., Kallio 2006; Thrane et al. 2014). The values of $a_{CDOM}(400)$ of the reference lakes were converted from water color values with an equation $a_{CDOM}(400) = 1.14 + 0.11\text{color}$ (Supporting Information Fig. S1) derived from the sampled lakes.

The absorption coefficients of total particles ($a_p(\lambda)$) were determined from filters with particles according to "Measurement of filter pad absorption inside an integrating sphere"-method (IOCCG 2018). The filters were stored in separate petri dishes and kept frozen (−80°C) until the analyses of $a_p(\lambda)$. The storage time of the filters varied from a few weeks up to 5 years. The effect of storage time of filters on the absorption of particles was non-significant according to an assessment explained in Data S1. The filters with particles and the blank filters were water-saturated for the measurements of optical density inside a 150-mm integrating sphere connected to a PerkinElmer Lambda™ 650 UV/Vis spectrophotometer using 2-nm slits at 1 nm-intervals. The absorption coefficient of phytoplankton pigments ($a_{phyto}(\lambda)$) (m^{-1}) was calculated as the difference between $a_p(\lambda)$ and the absorption coefficient of non-algal particles ($a_{NAP}(\lambda)$; m^{-1}):

$$a_{phyto}(\lambda) = a_p(\lambda) - a_{NAP}(\lambda) \quad (2)$$

The values of $a_{NAP}(\lambda)$ were determined like $a_p(\lambda)$ after extracting algal pigments from particles on filter with hot ethanol method (SFS 5772).

The spectral absorption coefficient for pure water ($aH_2O(\lambda)$) was derived from Neeley and Mannino (IOCCG, 2018) and interpolated to 1 nm spectral resolution with a spline function in Matlab. Total absorption coefficient spectrum was calculated as a sum of the absorption coefficients of CDOM, NAP, H_2O, and phytoplankton:

$$a_{tot}(\lambda) = a_{CDOM}(\lambda) + a_{NAP}(\lambda) + a_{phyto}(\lambda) + a_{H2O}(\lambda) \quad (3)$$

Determination of PUR/PAR

The fraction of PUR absorbed by phytoplankton over the entire water column from the PAR entering the lake (i.e., PUR/PAR) was determined as:

$$\frac{PUR}{PAR} = \frac{\sum Q_{abs,phyto,z=0-\infty}(\lambda)}{\sum Q_{d,z=0-}(\lambda)} \quad (4)$$

where $\Sigma Q_{abs,phyto,z=0-\infty}(\lambda)$ is the absorption of photons by phytoplankton in the whole water column (mol m^{-2} d^{-1} nm^{-1}) summed over the PAR spectrum (termed PUR) and $\Sigma Q_{d,z=0-}(\lambda)$ is the daily spectral downward photon flux density right below the water surface (mol m^{-2} d^{-1} nm^{-1}) summed over the PAR spectrum (termed PAR). $Q_{d,z=0-}(\lambda)$ was the ASTM G173-03 irradiance reference spectrum (Apell and McNeill 2019; SMARTS 2020). The absorption of photons by phytoplankton over the whole water column was calculated as:

$$Q_{abs,phyto,z=0-\infty}(\lambda) = Q_{d,z=0-}(\lambda)\frac{a_{phyto}(\lambda)}{a_{tot}(\lambda)} \quad (5)$$

The rationale and assumptions for the determination of PUR/PAR are explained in Data S1. Note that the determination of PUR/PAR is independent on the intensity of $Q_{d,z=0-}(\lambda)$.

Statistical methods

Statistical analyses were used for three purposes: (1) to assess the major water quality parameters affecting PUR/PAR in the sampled lakes, (2) to estimate the variability of PUR/PAR in the reference lakes based on their water quality, and (3) to estimate the impact of browning on PUR/PAR in a typical boreal lake.

We applied a regression analysis to examine the major determinants of PUR/PAR ratio in the sampled lakes along a CDOM-gradient. The dependency of the PUR/PAR value on $a_{CDOM}(400)$ and Chl *a*, tot-P, or tot-N concentrations was tested with competing logarithmic models (details in Data S1). We selected logarithmic models because the selected variables commonly display non-linear relationships (Nürnberg and Shaw 1998; Webster et al. 2008; Thrane et al. 2014). The eight competing models included explanatory variables separately, together, or through their interaction (Data S1). The most parsimonious model was selected based on the Akaike information criterion.

The most parsimonious model was applied to estimate PUR/PAR values in the 2250 reference lakes based on their water quality measures. To estimate a change in PUR/PAR values along a CDOM gradient in typical boreal lakes, we predicted PUR/PAR-values based on the average water quality at nine percentile bands of $a_{CDOM}(400)$: 5–15th, 15–25th, 25–35th, 35–45th, 45–55th, 55–65th, 65–75th, 75–85th, and 85–95th percentile, covering 90% of the reference lakes.

Finally, we estimated the response of PUR/PAR to browning expressed as an increase of $a_{CDOM}(400)$ value by 25%, 50%, 75% and 100%, which are examples of browning detected in the past decades and what could also happen in the future (Williamson et al. 2015; Räike et al. 2016; Kritzberg 2017; Lepistö et al. 2021). For the estimations, we selected a typical boreal lake according to a median value of $a_{CDOM}(400)$ in the reference lakes. The impact of browning was assessed as a typical development of PUR/PAR-values in the reference lakes described by the most parsimonious model. All statistical analyses and data processing were performed using R software (R Core Team 2022, version 4.2.1).

Table 1. Min, max, mean, and median values as well as 5th, 25th, 75th, and 95th percentiles of the lake morphometry and water quality among the 128 sampled lakes. Lakes are characterized by lake area (km^2), lake volume (million m^3, Mm^3), max and mean depths (m), concentrations of total nitrogen and phosphorus ($\mu g\ L^{-1}$), Chl *a* concentration ($\mu g\ L^{-1}$), color value (mg Pt L^{-1}), $a_{CDOM}(400)$ value (m^{-1}), and DOC concentration (mg L^{-1}).

Parameter	Min–max	Mean	Median	5th	25th	75th	95th
Lake area (km^2)	0.009–894	61	15.2	1.0	6.1	48	229
Lake vol (Mm^3)	2–12195	636	88	6	26	451	2201
Max depth (m)	2.3–94	31	25	6.0	12	44	85
Mean depth (m)	0.6–23	6.4	5.4	1.9	3.3	8.5	16
The tot-N ($\mu g\ L^{-1}$)	115–1503	560	519	290	416	630	1010
The tot-P ($\mu g\ L^{-1}$)	3–173	23	16	5	8	26	78
Chl *a* ($\mu g\ L^{-1}$)	1–77	11	7	2	4	14	34
$a_{CDOM}(400)$ (m^{-1})	1.2–35.2	9.7	6.9	2.2	4.5	13.3	24.7
Color (mg Pt L^{-1})	13–240	77	56	20	38	103	188
DOC (mg L^{-1})	1.8–24.4	10.5	10.1	4.9	8.3	12.5	17.0

Results

Water quality and morphometry of the study lakes

Regarding water quality, 90% of the 128 sampled lakes from 5th to 95th percentile covered tot-N range 290–1010 $\mu g\ L^{-1}$, tot-P range 5–78 $\mu g\ L^{-1}$, Chl *a* range 2–34 $\mu g\ L^{-1}$, and $a_{CDOM}(400)$ range 2–25 m^{-1} (Table 1; Fig. 1). In addition, DOC concentration ranged from 5 to 17 mg L^{-1} among 90% of the sampled lakes. In comparison, 90% of the 2250 reference lakes covered ranges in tot-N of 255–1032 $\mu g\ L^{-1}$, tot-P of 5–66 $\mu g\ L^{-1}$, Chl *a* of 2–40 $\mu g\ L^{-1}$, $a_{CDOM}(400)$ of 2–26 m^{-1}, and DOC of 5 to 22 mg L^{-1} (Table 2). Concerning lake morphometry, 90% of the sampled lakes represented ranges in lake area of 1–229 km^2, lake volume of 6–2200 million m^3 (Mm^3) and mean depth of 2–16 m (Table 1). Respectively, 90% of the reference lakes covered lake area range 0.4–30.8 km^2, lake volume range 0.9–287 Mm^3 and mean depth range 1–9 m (Table 2). Large lakes were overrepresented among the sampled lakes compared to the reference lakes. However, the water quality of the sampled lakes represented well that of the reference lakes, and hence boreal lakes in general.

Absorption of PAR in the sampled lakes

For each sampled lake, we determined the spectral absorption coefficient for CDOM, H_2O, non-algal particles and phytoplankton as illustrated for Lake Jyväsjärvi in Fig. 2a. Each absorption coefficient was divided by the total absorption coefficient as illustrated for a_{phyto}/a_{tot} in Fig. 2b. These ratios were multiplied with the spectral PAR entering the lake (Fig. 2c) to calculate the spectral PAR absorbed by each absorbing component in the entire water column, as illustrated for phytoplankton in Fig. 2d. Finally, the photons absorbed by each absorption component over the wavelength range 400–700 nm were divided by the PAR entering the lake for the fraction of PAR absorbed by each absorbing component like shown for phytoplankton as a

Table 2. Min, max, mean, and median values as well as 5th, 25th, 75th, and 95th percentiles of the lake morphometry and water quality among the 2250 reference boreal lakes. Lakes are characterized by lake area (km^2), lake volume (million m^3, Mm^3), max and mean depths (m), concentrations of total nitrogen and phosphorus ($\mu g\ L^{-1}$), Chl *a* concentration ($\mu g\ L^{-1}$), color value (mg Pt L^{-1}), $a_{CDOM}(400)$ value (m^{-1}), and DOC concentration (mg L^{-1}).

Parameter	Min–max	Mean	Median	5th	25th	75th	95th
Lake area (km^2)	0.02–1377	10	1.5	0.4	0.8	4	31
Lake vol (Mm^3)	0.04–14822	98	6	0.9	3	21	287
Max depth (m)	0.7–94	16	12	2	7	21	42
Mean depth (m)	0.2–23	4	4	1	2	5	9
The tot-N ($\mu g\ L^{-1}$)	97–2725	542	477	255	369	642	1032
The tot-P ($\mu g\ L^{-1}$)	1–209	24	18	5	11	29	66
Chl *a* ($\mu g\ L^{-1}$)	0.5–310	14	8	2	5	16	40
Color (mg Pt L^{-1})	2–375	87	70	17	40	120	208
a_{CDOM} (400) (m^{-1})	0.3–46.5	10.8	8.9	2.1	5.0	14.9	25.8
DOC (mg L^{-1})	3.7–36.3	11.1	9.7	5.0	7.1	14.0	21.7

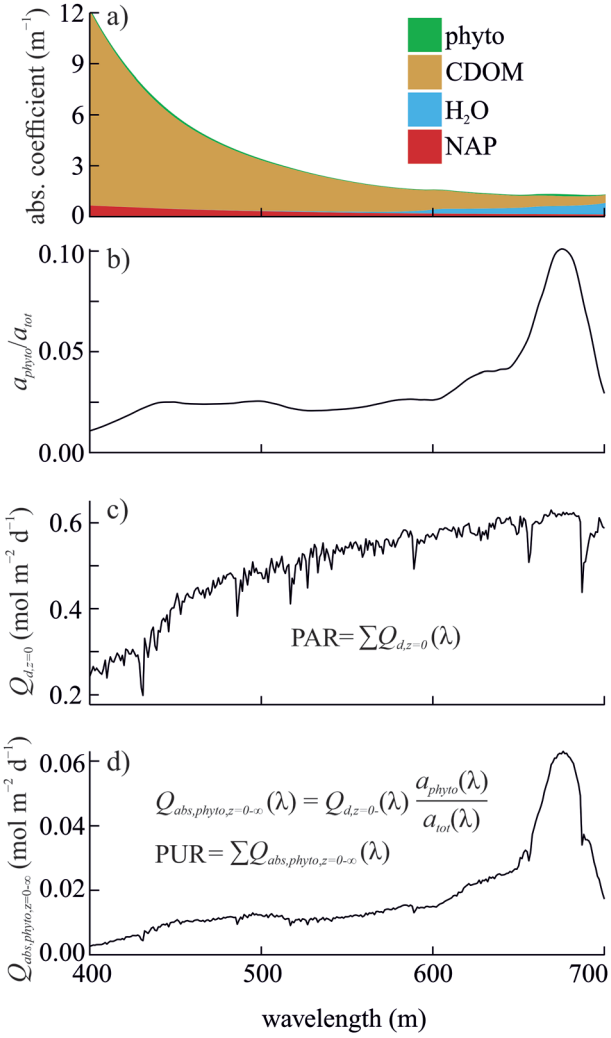

Fig. 2. A graphical visualization of determining PUR from the PAR in Lake Jyväsjärvi. Panel (**a**) shows the spectral absorption coefficients of phytoplankton, CDOM, H_2O, and NAP. Panel (**b**) shows the ratio of spectral absorption coefficients, phytoplankton ($a_{phyto}(\lambda)$) to the total absorption ($a_{tot}(\lambda)$). Panel (**c**) shows the spectral photon flux density of PAR just below the water surface. Panel (**d**) shows spectral PUR determined over the whole water column. The PUR summed over the wavelengths of 400–700 nm was used to calculate PUR/PAR (Eq. 4).

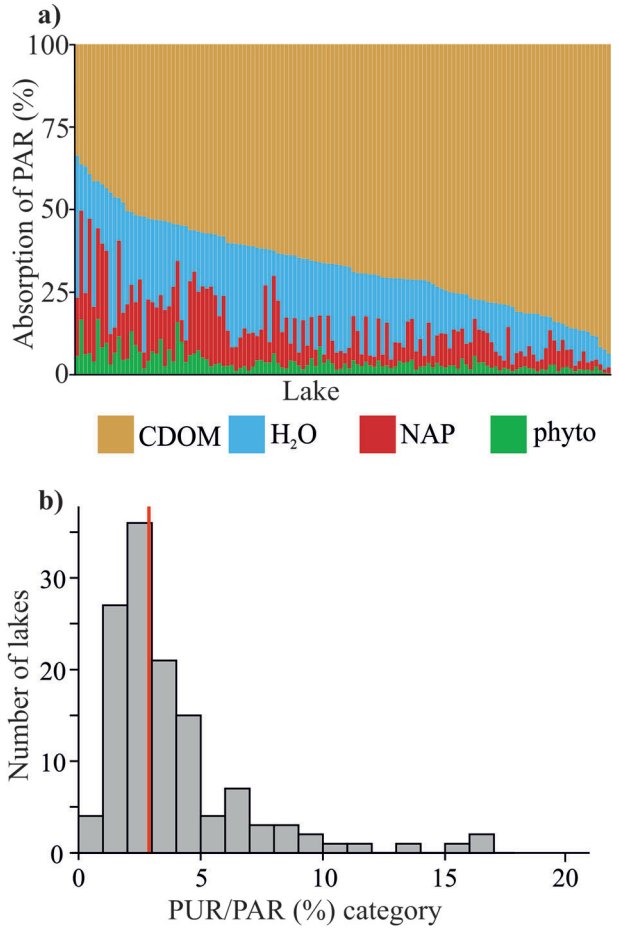

Fig. 3. The percentage of incoming PAR absorbed by (**a**) the four components and (**b**) phytoplankton in the 128 sampled lakes. In (a) the barplot shows the relative absorption of PAR by CDOM, H_2O, NAP, and phytoplankton (phyto, i.e., PUR/PAR) in each sampled lake. In (b) the histogram shows the variation in PUR/PAR values, with the vertical red line indicating the median value.

PUR/PAR ratio (Eq. 4). The fraction of PAR absorbed by phytoplankton over the whole water column (i.e., PUR/PAR) was 0.4–17% (median 3%) in the sampled lakes (Figs. 3, 4a). In most of the sampled lakes, CDOM was the largest absorbing component, absorbing 33–94% of the incident PAR (Fig. 3a). The fractions of PAR absorbed by non-algal particles and H_2O absorption were 1–40% and 3–43%, respectively (Fig. 3a).

The major water quality predictors of PUR/PAR in the sampled lakes

We used regression analyses to explore how the PUR/PAR values depended on CDOM and Chl *a*, tot-P or tot-N in competing logarithmic models (Supporting Information Tables S2–S4). Among the competing models, three models were equally good and each explained 52% of the variability in logarithmic PUR/PAR values: (1) a model including $a_{CDOM}(400)$ and Chl *a* as individual predictors (model 5 in Supporting Information Table S2; Fig. 4a,b); (2) a full model including $a_{CDOM}(400)$, Chl *a* and their interaction term (model 8 in Supporting Information Table S2); and (3) a model including tot-P and an interaction term of tot-P and $a_{CDOM}(400)$ (model 7 in Table S3; model equations in Data S1). In the three best models, the regression coefficient of $a_{CDOM}(400)$ was negative and the regression coefficient of Chl *a* or tot-P was positive (Supporting Information Table S2, S3). Model 8 (Supporting Information Table S2) had one non-significant parameter and thus was set aside. Among the two remaining, equally good models, model 5 (Supporting Information Table S2)

was selected for further examination due to its simpler structure compared to model 7 (Supporting Information Table S3).

Estimation of PUR/PAR values in the reference lakes

The model 5 (Supporting Information Table S2) was selected to predict PUR/PAR values in the reference lakes based on their $a_{CDOM}(400)$ and Chl *a* concentration (Supporting Information Table S2; Fig. 4a,b). The logarithmic model 5 was converted to a linear scale:

$$\frac{PUR}{PAR} = a_{CDOM}(400)^{-0.645} \times Chl\,a^{0.552} \times e^{-3.288} \quad (6)$$

and illustrated as surfaces in Fig. 4a,b. According to Eq. 6, the values of PUR/PAR varied from 0.5% to 20% with a median of 3% in the reference lakes (Fig. 5).

To estimate a typical range of PUR/PAR values in most boreal lakes, PUR/PAR values were calculated (Eq. 6) for the reference lakes based on their concentration of Chl *a* along a CDOM gradient from 5 to 15th and 85 to 95th percentile bands of $a_{CDOM}(400)$. Chl *a* concentration for each centered $a_{CDOM}(400)$ percentile band was determined based on a logarithmic dependence between the variables in the reference lakes ($Chl\,a = 1.80 a_{CDOM}(400)^{0.75}$, adj. $R^2 = 0.29$; Fig. 4d; Supporting Information Fig. S2). The PUR/PAR value was on average 3.8% for the 5–15th percentile band of $a_{CDOM}(400)$ centered at 3.8 m^{-1} and decreased to on average 2.5% for the 85–95th percentile band of $a_{CDOM}(400)$ centered at 20 m^{-1} (Fig. 4b,c; Supporting Information Table S5). Along the same gradient, the mean concentration of Chl *a* more than tripled, as the values increased from 5 to 17 $\mu g\,L^{-1}$ (Supporting Information Table S5; Fig. S2; Fig. 4b,d). Both total nitrogen and phosphorus concentrations increased with CDOM content in the reference lakes (Supporting Information Fig. S3). In addition, an increase in the CDOM content decreased PUR/PAR values more in low-CDOM than in high-CDOM lakes (Fig. 4a–c).

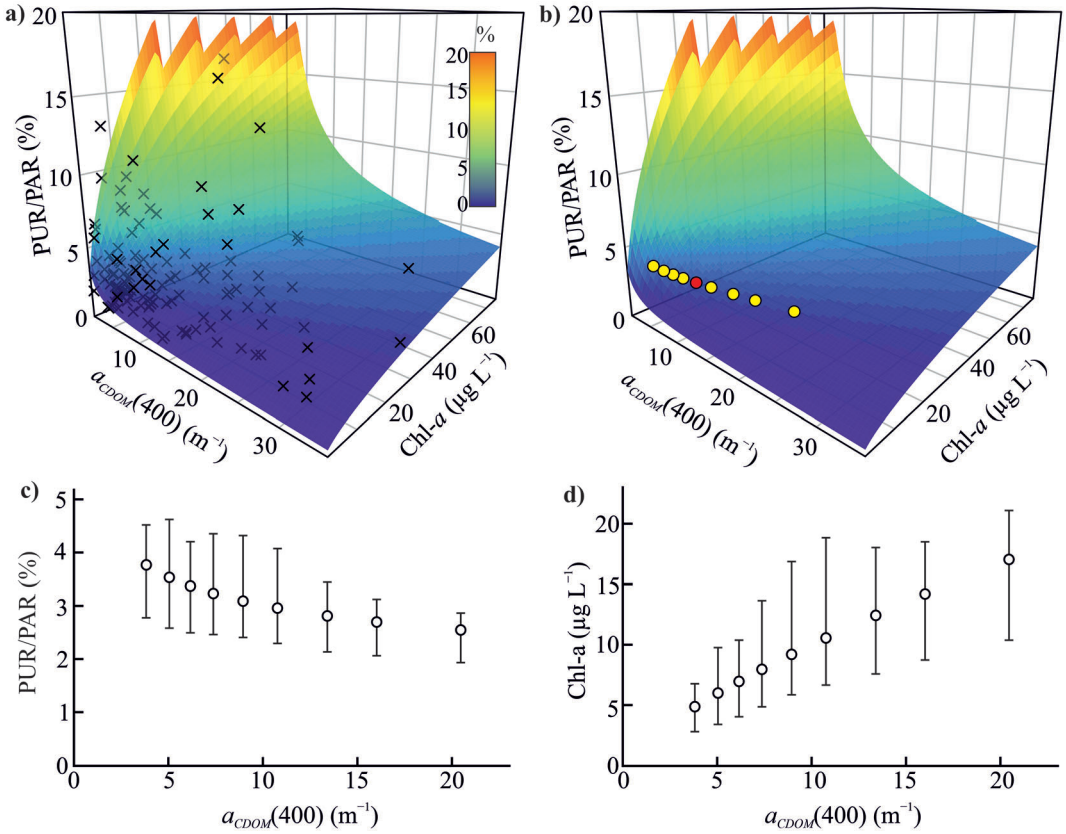

Fig. 4. Graphs showing the dependency of the fraction of PAR absorbed by phytoplankton (PUR/PAR, %) on $a_{CDOM}(400)$ and Chl *a* (**a**–**c**), and Chl *a* (**d**) on $a_{CDOM}(400)$ value. The 3D surfaces in (a and b) show calculated PUR/PAR (model 5 in Supporting Information Table S2) based on $a_{CDOM}(400)$ and Chl *a*, a color scale indicating the PUR/PAR value. Ticks (a) show the datapoints in the sampled lakes, and yellow dots (b) show the predicted PUR/PAR according to the nine centered percentile bands of $a_{CDOM}(400)$ from 5 to 15th to 85 to 95th percentile and corresponding Chl *a* values in the reference lakes (Supporting Information Table S5; Fig. S2). The red point (b) shows a median boreal lake according to $a_{CDOM}(400)$. The dots in (c and d) show the calculated PUR/PAR values (model 5 in Supporting Information Table S2) and Chl *a* concentrations based on measured values (Supporting Information Fig. S2), respectively, with the centered percentile bands of $a_{CDOM}(400)$ in the reference lakes. The error bars in (c and d) indicate the first and third quartiles of PUR/PAR and Chl *a* in each percentile band.

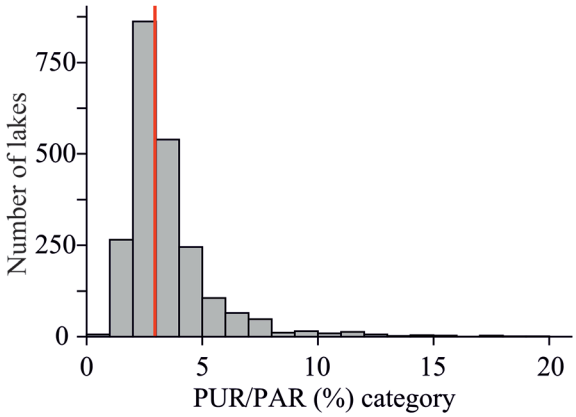

Fig. 5. A histogram of the variation in the percentage of photosynthetically active radiation absorbed by phytoplankton (PUR/PAR) calculated using model 5 in Supporting Information Table S2 in the 2250 reference boreal lakes. The vertical red line indicates the median value.

Predicting the impact of browning on PUR/PAR values

The impact of browning on PUR/PAR values was estimated for the median reference lake (PUR/PAR = 3.1%, $a_{CDOM}(400) = 8.9\ m^{-1}$ and Chl $a = 9.2\ \mu g\ L^{-1}$, Fig. 4b–d, Supporting Information Table S6). Our browning scenario assumed not only an increase in the CDOM content but also an increase in the Chl *a* concentrations as found in the reference lakes along the CDOM gradient (Supporting Information Figs. S2, S3; Supporting Information Table S7). In terms of nutrients, the browning scenario assumed that water quality of the median lake will change according to the ratios 1.4 μg tot-P/m^{-1} $a_{CDOM}(400)$, 1.8 μg tot-P/mg DOC and 0.15 μg tot-P/mg Pt with increasing allochthonous input (Supporting Information Table S7). Browning causing a 25% increase in the $a_{CDOM}(400)$ value and an increase in Chl *a* concentration to 10.9 $\mu g\ L^{-1}$ of the median boreal lake was predicted to decrease PUR/PAR to 2.9% (Fig. 4c,d; Supporting Information Table S6). PUR/PAR-values were predicted to decrease to 2.8%, 2.7% and 2.6% but Chl *a* concentrations to increase to 12.4, 14.0 and 15.4 $\mu g\ L^{-1}$ with 50%, 75% and 100% increases, respectively, in $a_{CDOM}(400)$. Thus, although CDOM decreases PUR/PAR values according to the model 5, the severity of the decrease was partly compensated by an assumed increase of Chl *a* concentration. Due to this compensation, the predicted decrease in PUR/PAR values was only moderate for a typical range of browning reported in the recent decades.

Discussion

This study quantifies the decrease in the fraction of PAR absorbed by phytoplankton over the whole water column (i.e., PUR/PAR) as a function of increasing CDOM content in boreal lakes. We show that phytoplankton generally makes a low contribution to the absorption of PAR in boreal lakes, whereas CDOM absorbs most of the PAR in the water column. The PUR/PAR value in the sampled lakes is best predicted by a logarithmic model including CDOM content (quantified as $a_{CDOM}(400)$) and Chl *a* concentration as explanatory variables. Based on the model, an increase of CDOM content decreases PUR/PAR but a concurrent increase in the Chl *a* concentration with the CDOM partly compensates for the decline of the PUR/PAR in boreal lakes along a CDOM gradient. Assuming that browning increases both CDOM content and Chl *a* concentration as in the reference lakes, our model suggests that the reported degree of browning decreases the PUR/PAR values in typical boreal lakes only moderately.

The fraction of PAR absorbed by phytoplankton

The range (0.4–17%) and median (3%) of PUR/PAR values in our sampled boreal lakes are lower than values of a similar parameter a_{phyto}/a_{tot} reported previously for Scandinavian lakes (range 2.2–28.2% and median 6.6%; Thrane et al. 2014) and for a Canadian reservoir (range 2–8% and mean 5%; Watanabe et al. 2015). In our study lakes, the upper ranges of CDOM content ($a_{CDOM}(400)$ 1.2–32.5 m^{-1}) and DOC (1.8–24.4 mg L^{-1}) exceed those reported for boreal lakes in earlier studies, such as by Thrane et al. (2014) ($a_{CDOM}(400)$ 0.1–15 m^{-1} and DOC 0.3–12.3 mg L^{-1}), by Kutser et al. (2005) ($a_{CDOM}(420)$ 1.2–7.7 m^{-1} and DOC 7–12 mg L^{-1}), or by Ylöstalo et al. (2014) ($a_{CDOM}(420) \sim$ 1–7 m^{-1} and DOC 5.1–11.2 mg L^{-1}). Thus, the high content of CDOM and DOC in our study lakes likely explain the low values of PUR/PAR, owing to the strong absorption of PAR by CDOM. In general, PUR/PAR values are low in boreal lakes, where CDOM is the dominant absorbing component in most lakes (Thrane et al. 2014; our study).

The impact of CDOM, nutrients, and Chl *a* on PUR/PAR in lakes along a CDOM gradient

Our regression models indicate that CDOM affects the PUR/PAR value negatively, while nutrients and Chl *a* have a positive impact on PUR/PAR. In a similar model applied to Scandinavian lakes, tot-P and DOC increased and decreased the light absorption by phytoplankton pigments, respectively (Thrane et al. 2014). Several factors can explain the findings of the models (this study; Thrane et al. 2014). An increase in CDOM content or the chromophores of DOC decrease the fraction of PAR absorbed by phytoplankton because they compete for available photons with phytoplankton (Kirk 2011; Solomon et al. 2015). On the other hand, nutrients, such as tot-P, can increase the biomass of phytoplankton, Chl *a* concentrations, and hence the light absorption by phytoplankton (Marzetz et al. 2020). Nutrients and DOC often increase concurrently with CDOM in lakes (Thrane et al. 2014; Seekell et al. 2015; Hamdan et al. 2021; this study). The carbon in DOC can supply energy and the carbon metabolites for mixotrophic phytoplankton, increasing their biomass and light absorption in high-CDOM lakes (Calderini et al. 2022). Further, phytoplankton can increase

their cellular Chl *a* content as a response to lowered light availability and this photoacclimation can increase the light absorption without a similar increase in biovolume (Fennel and Boss 2003; Sherbo et al. 2023). All in all, in lakes along a CDOM gradient, the shading effect of chromophores of DOM can be partly compensated by higher concentration of phytoplankton pigments related to better availability of nutrients (tot-P) and carbon (DOC) or photoacclimation (this study; Thrane et al. 2014; Calderini et al. 2022; Sherbo et al. 2023).

The effect of browning on the PUR/PAR values

Our study suggests that an increase of $a_{CDOM}(400)$ by 25–100% in lake water does reduce PUR/PAR values, but only rather modestly (5–15%) when accounting for the typical development of Chl *a* in 2250 boreal lakes with increasing CDOM captured in our models. Our browning scenario assumes that browning increases not only the CDOM content but also elevates the nutrient and Chl *a* concentrations in lakes. Our scenario is consistent with the reported concomitant increase of nutrient concentrations and CDOM or DOC content associated with browning (e.g., Corman et al. 2018; Lepistö et al. 2021). A key feature of our scenario is that it involves the possible adaptations of phytoplankton (e.g., photoacclimation) to elevated CDOM as found on average in the 2250 reference lakes. However, our scenario is based on spatial differences among lakes and their catchments along a CDOM-gradient (a space-for-time assumption), rather than on actual temporal responses of PUR/PAR to an increasing allochthonous loading in individual lakes because of the lack of such data (Stetler et al. 2021). Our browning scenario describes a typical response in PUR/PAR values on average across boreal catchments, whereas the response of an individual lake may be different depending on the characteristics of the catchment and the factors causing browning (e.g., recovery of acidification, changes in land use or vegetation).

Individual lake responses of PUR/PAR values to browning may differ from the average modeled response based on our browning scenario. One factor that influences PUR/PAR-values in lakes experiencing browning is the nutrient to CDOM ratio of the increased allochthonous loading (Kelly et al. 2018). In this study, we assumed that browning in lakes takes place with the water quality changes characterized by the ratios 1.8 μg tot-P/mg DOC, 1.4 μg tot-P/m^{-1} $a_{CDOM}(400)$, and 0.15 μg tot-P/mg Pt color as found on average in the 2250 reference lakes along a CDOM gradient. In our reference lakes, the tot-P/DOC ratio is higher than that reported elsewhere for allochthonous loading from terrestrial boreal forest catchments (0.5–1.2 μg tot-P/mg DOC; Jansson et al. 2012; Finér et al. 2021) but lower than soil leachates in the catchments of browned lakes in the temperate region (6–15 μg tot-P/mg DOC; Corman et al. 2018). The loading from Swedish forest streams has been characterized by 0.05 μg tot-P/mg Pt-color (Meili 1992), which is lower than the corresponding mean ratio in our reference lakes. In boreal lakes, browning may decrease PUR/PAR values more than estimated in this study if their elevated allochthonous loading has lower nutrient to CDOM ratios than in our reference lakes. However, it is not simple to predict the responses of PUR/PAR to browning based solely on the characteristics of allochthonous loading because the responses happen within the receiving lakes. For example, the cycling of allochthonous tot-P is complicated in lakes; solar radiation can quickly break down a part of CDOM (photobleaching) and phytoplankton can adapt (mixotrophy and photoacclimation) to changing environmental conditions (Del Vecchio and Blough 2002; Vähätalo and Wetzel 2004). In this study, we evaluated the response of PUR/PAR to browning based on changes found in large number of lakes along a CDOM gradient, but we encourage future research into the quality of increased allochthonous matter as an explainer of PUR/PAR values in browning lakes.

Conclusions

Owing to the high content of CDOM in many boreal lakes, the contribution of phytoplankton to the absorption of incident PAR in boreal lakes is low, while CDOM absorbs most of the light over the whole water column. Our results show that the light absorption by phytoplankton decreases with increasing CDOM content, whereas Chl *a* concentration tends to concurrently increase with CDOM, partly compensating the negative effect of the CDOM on the PUR/PAR values. Assuming that browning increases both CDOM and Chl *a* contents of a lake, our model suggests that the decrease in the light absorption by phytoplankton in response to typical browning of most boreal lakes is only moderate, owing to either/or a combination of photoacclimation of phytoplankton to lowered light supply and increased nutrient concentrations associated with allochthonous matter in high-CDOM lakes.

Data availability statement

The data that support the findings of this study are available from the corresponding author upon reasonable request.

References

Ahonen, S. A., J. Seppälä, J. S. Karjalainen, J. Kuha, and A. V. Vähätalo. 2023. Increasing air temperature relative to water temperature makes the mixed layer shallower, reducing phytoplankton biomass in a stratified lake. Freshwater Biol. **68**: 1–11. doi:10.1111/fwb.14048

Apell, J. N., and K. McNeill. 2019. Updated and validated solar irradiance reference spectra for estimating environmental photodegradation rates. Environ. Sci. Proc. Imp. **21**: 427–437. doi:10.1039/c8em00478a

Ask, J., J. Karlsson, and M. Jansson. 2012. Net ecosystem production in clear-water and brown-water lakes. Global Biogeochem. Cycles **26**: GB1017. doi:10.1029/2010GB003951

Bergström, A. K., and J. Karlsson. 2019. Light and nutrient control phytoplankton biomass responses to global change

in northern lakes. Glob. Change Biol. **25**: 2021–2029. doi:10.1111/gcb.14623

Calderini, M. L., P. Salmi, C. Rigaud, E. Peltomaa, and S. J. Taipale. 2022. Metabolic plasticity of mixotrophic algae is key for their persistence in browning environments. Mol. Ecol. **31**: 4726–4738. doi:10.1111/mec.16619

Chambers, P. A., and J. Kalff. 1985. Depth distribution and biomass of submersed aquatic macrophyte communities in relation to secchi depth. Can. J. Fish. Aquat. Sci. **42**: 701–709. doi:10.1139/f85-090

Corman, J. R., B. L. Bertolet, N. J. Casson, S. D. Sebestyen, R. K. Kolka, and E. H. Stanley. 2018. Nitrogen and phosphorus loads to temperate seepage lakes associated with allochthonous dissolved organic carbon loads. Geophys. Res. Lett. **45**: 5481–5490. doi:10.1029/2018GL077219

Daniels, W. C., G. W. Kling, and E. E. Giblin. 2015. Benthic community metabolism in deep and shallow Arctic lakes during 13 years of whole-lake fertilization. Limnol. Oceanogr. **60**: 1604–1618. doi:10.1002/lno.10120

de Wit, H. A., and others. 2016. Current browning of surface waters will be further promoted by wetter climate. Environ. Sci. Tech. Let. **3**: 430–435. doi:10.1021/acs.estlett.6b00396

Del Vecchio, R., and N. V. Blough. 2002. Photobleaching of chromophoric dissolved organic matter in natural waters: Kinetics and modelling. Mar. Chem. **78**: 231–253. doi:10.1016/S0304-4203(02)00036-1

Evans, C. D., P. J. Chapman, J. M. Clark, D. T. Monteith, and M. S. Cresser. 2006. Alternative explanations for rising dissolved organic carbon export from organic soils. Glob. Change Biol. **12**: 2044–2053. doi:10.1111/j.1365-2486.2006.01241.x

Fennel, K., and E. Boss. 2003. Subsurface maxima of phytoplankton and chlorophyll: Steady-state solutions from a simple model. Limnol. Oceanogr. **48**: 1521–1534. doi:10.4319/lo.2003.48.4.1521

Finér, L., and others. 2021. Drainage for forestry increases N, P and TOC export to boreal surface waters. Sci. Total Environ. **762**: 144098. doi:10.1016/J.SCITOTENV.2020.144098

Hamdan, M., P. Byström, E. R. Hotchkiss, M. J. Al-Haidarey, and J. Karlsson. 2021. An experimental test of climate change effects in northern lakes: Increasing allochthonous organic matter and warming alters autumn primary production. Freshwater Biol. **66**: 815–825. doi:10.1111/fwb.13679

IOCCG. 2018. IOCCG Ocean optics and biogeochemistry protocols for Satellite Ocean colour sensor validation, p. 78. *In* A. R. Neeley and A. Mannino [eds.], Inherent optical property measurements and protocols: Absorption coefficient, v. **1.0**. International Ocean-Colour Coordinating Group (IOCCG). doi:10.25607/OBP-119

ISO/DIS 15681–2. 2005. Water quality–Determination of orthophosphate and total phosphorus by flow analysis (FIA and CFA)-Part2: Method by continuous flow analysis (CFA).

Jansson, M., M. Breggren, H. Laudon, and A. Jonsson. 2012. Bioavailable phosphorus in humic headwater streams in boreal Sweden. Limnol. Oceanogr. **57**: 1161–1170. doi:10.4319/lo.2012.57.4.1161

Jones, R. I., and L. Arvola. 1984. Light penetration and some related characteristics in small forest lakes in southern Finland. Verh. Internat. Verein. Limnol. **22**: 811–816. doi:10.1080/03680770.1983.11897390

Kallio, K. 2006. Optical properties of Finnish lakes estimated with simple bio-optical models and water quality monitoring data. Nord. Hydrol. **37**: 183–204. doi:10.2166/nh.2006.0014

Karlsson, J., P. Byström, J. Ask, P. Ask, L. Persson, and M. Jansson. 2009. Light limitation of nutrient-poor lake ecosystems. Nature **460**: 506–509. doi:10.1038/nature08179

Kelly, P. T., C. T. Solomon, J. A. Zwart, and S. E. Jones. 2018. A framework for understanding variation in pelagic gross primary production of lake ecosystems. Ecosystems **21**: 1364–1376. doi:10.1007/s10021-018-0226-4

Kirk, J. T. O. 2011. Light and photosynthesis in aquatic ecosystems, 3rd ed. Cambridge Univ. Press, p. 61–90.

Kortelainen, P. 1993. Content of total organic carbon in Finnish lakes and its relationship to catchment characteristics. Can. J. Fish. Aquat. Sci. **50**: 1477–1483. doi:10.1139/f93-168

Kritzberg, E. S. 2017. Centennial-long trends of lake browning show major effect of afforestation. Limnol. Oceanogr. Lett **2**: 105–112. doi:10.1002/lol2.10041

Kritzberg, E. S., and S. M. Ekström. 2012. Increasing iron concentrations in surface waters–a factor behind brownification? Biogeosciences **9**: 1465–1478. doi:10.5194/bg-9-1465-2012

Kutser, T., D. C. Pierson, L. Tranvik, A. Reinart, S. Sobek, and K. Kallio. 2005. Using satellite remote sensing to estimate the colored dissolved organic matter absorption coefficient in lakes. Ecosystems **8**: 709–720. doi:10.1007/s10021-003-0148-6

Lenard, T., and W. Ejankowski. 2017. Natural water brownification as a shift in the phytoplankton community in a deep hard water lake. Hydrobiologia **787**: 153–166. doi:10.1007/s10750-016-2954-9

Lepistö, A., A. Räike, T. Sallantaus, and L. Finér. 2021. Increases in organic carbon and nitrogen concentrations in boreal forested catchments—Changes driven by climate and deposition. Sci. Total Environ. **780**: 146627. doi:10.1016/j.scitotenv.2021.146627

Majasalmi, T., M. Rautiainen, and P. Stenberg. 2014. Modelled and measured fPAR in a boreal forest: Validation and application of a new model. Agric. For. Meteorol. **189–190**: 118–124. doi:10.1016/j.agrformet.2014.01.015

Marzetz, V., E. Spijkerman, M. Striebel, and A. Wacker. 2020. Phytoplankton community responses to interactions between light intensity, light variations, and phosphorus supply. Front. Environ. Sci. **8**: 539733. doi:10.3389/fenvs.2020.539733

Meili, M. 1992. Sources, concentrations and characteristics of organic matter in softwater lakes and streams of the

Swedish forest region. Hydrobiologia **229**: 23–41. doi:10.1007/BF00006988

Monteith, D. T., and others. 2007. Dissolved organic carbon trends resulting from changes in atmospheric deposition chemistry. Nature **450**: 537–540. doi:10.1038/nature06316

Morel, A. 1978. Available, usable, and stored radiant energy in relation to marine photosynthesis. Deep-Sea Res. **25**: 673–688. doi:10.1016/0146-6291(78)90623-9

Murray, C., S. Markager, C. A. Stedmon, T. Juul-Pedersen, M. K. Sejr, and A. Bruhn. 2015. The influence of glacial melt water on bio-optical properties in two contrasting Greenlandic fjords. Estuar. Coast. Shelf Sci. **163**: 72–83. doi:10.1016/j.ecss.2015.05.041

Naumann, E. 1929. The scope and chief problems of regional limnology. Int. Rev. Hydrobiol. **22**: 423–444. doi:10.1002/iroh.19290220128

Nieminen, M., S. Sarkkola, T. Sallantaus, E. M. Hasselquist, and H. Laudon. 2021. Peatland drainage–a missing link behind increasing TOC concentrations in waters from high latitude forest catchments? Sci. Total Environ. **774**: 145150. doi:10.1016/j.scitotenv.2021.145150

Nürnberg, G. K., and M. Shaw. 1998. Productivity of clear and humic lakes: Nutrients, phytoplankton, bacteria. Hydrobiologia **382**: 97–112. doi:10.1023/A:1003445406964

R Core Team. 2022. R: A language and environment for statistical computing. R Foundation for Statistical Computing, https://www.R-project.org/

Reynolds, C. S., M. L. White, R. T. Clarke, and A. F. Marker. 1990. Suspension and settlement of particles in flowing water: Comparison of the effects of varying water depth and velocity in circulating channels. Freshwater Biol. **24**: 23–34. doi:10.1111/j.1365-2427.1990.tb00304.x

Räike, A., P. Kortelainen, T. Mattsson, and D. N. Thomas. 2016. Long-term trends (1975–2014) in the concentrations and export of carbon from Finnish rivers to the Baltic Sea: Organic and inorganic components compared. Aquat. Sci. **78**: 505–523. doi:10.1007/s00027-015-0451-2

Seekell, D. A., J.-F. Lapierre, and J. Karlsson. 2015. Trade-offs between light and nutrient availability across gradients of dissolved organic carbon concentration in Swedish lakes: Implications for patterns in primary production. Can. J. Fish. Aquat. Sci. **72**: 1663–1671. doi:10.1139/cjfas-2015-0187

SFS-EN ISO 11905-1. 1997. Water quality. Determination of nitrogen. Part 1: Method using oxidative digestion with peroxodisulfate.

SFS-ISO 10260. 1992. Water quality—Measurement of biochemical parameters—Spectrometric determination of the chlorophyll-a concentration. International Organization for Standardization.

SFS-EN ISO 7887. 2011. Water quality. *In* Examination and determination of colour. International Organization for Standardization.

Sherbo, B. A. H., J. Tonin, M. J. Paterson, B. J. Hann, J. Kozak, and S. N. Higgins. 2023. The effects of terrestrial dissolved organic matter on phytoplankton biomass and productivity in boreal lakes. Freshwater Biol. **68**: 1–11. doi:10.1111/fwb.14178

Siegel, D. A., S. Maritorena, N. B. Nelson, D. A. Hansell, and M. Lorenzi-Kayser. 2002. Global distribution and dynamics of colored dissolved and detrital organic materials. J. Geophys. Res. **107**: 1–14. doi:10.1029/2001JC000965

Škerlep, M., E. Steiner, A. L. Axelsson, and E. S. Kritzberg. 2020. Afforestation driving long-term surface water browning. Glob. Change Biol. **26**: 1390–1399. doi:10.1111/gcb.14891

SMARTS. 2020. ASTM G173-03 irradiance reference spectrum calculated using the Simple Model of the Atmospheric Radiative Transfer of Sunshine (SMARTS). https://www.nrel.gov/grid/solar-resource/spectra.html

Smith, R. C., J. Marra, M. J. Perry, K. S. Baker, E. Swift, E. Buskey, and D. A. Kiefer. 1989. Estimation of a photon budget for the upper ocean in the Sargasso Sea. Limnol. Oceanogr. **34**: 1673–1693. doi:10.4319/lo.1989.34.8.1673

Solomon, C. T., and others. 2015. Ecosystem consequences of changing inputs of terrestrial dissolved organic matter to lakes: Current knowledge and future challenges. Ecosystems **18**: 376–389. doi:10.1007/s10021-015-9848-y

Stetler, J. T., L. B. Knoll, C. T. Driscoll, and K. C. Rose. 2021. Lake browning generates a spatiotemporal mismatch between dissolved organic carbon and limiting nutrients. Limnol. Oceanogr. Lett. **6**: 182–191. doi:10.1002/lol2.10194

Strock, K. E., S. J. Nelson, J. S. Kahl, J. E. Saros, and W. H. McDowell. 2014. Decadal trends reveal recent acceleration in the rate of recovery from acidification in the northeastern U.S. Environ. Sci. Technol. **48**: 4681–4689. doi:10.1021/es404772n

Thrane, J.-E., D. O. Hessen, and T. Andersen. 2014. The absorption of light in lakes: Negative impact of dissolved organic carbon on primary productivity. Ecosystems **17**: 1040–1052. doi:10.1007/s10021-014-9776-2

Tranvik, L. J. 1990. Bacterioplankton growth on fractions of dissolved organic carbon of different molecular weights from humic and clear waters. Appl. Environ. Microbiol. **56**: 1672–1677. doi:10.1128/aem.56.6.1672-1677.1990

Vähätalo, A. V., and R. G. Wetzel. 2004. Photochemical and microbial decomposition of chromophoric dissolved organic matter during long (months–years) exposures. Mar. Chem. **89**: 313–326. doi:10.1016/j.marchem.2004.03.010

Watanabe, S., I. Laurion, S. Markager, and W. F. Vincent. 2015. Abiotic control of underwater light in a drinking water reservoir: Photon budget analysis and implications for water quality monitoring. Water Resour. Res. **51**: 6290–6310. doi:10.1002/2014WR015617

Webster, K. E., and others. 2008. An empirical evaluation of the nutrient-color paradigm for lakes. Limnol. Oceanogr. **53**: 1137–1148. doi:10.4319/lo.2008.53.3.1137

Williamson, C. E., E. P. Overholt, R. M. Pilla, T. H. Leach, J. A. Brentrup, L. B. Knoll, E. M. Mette, and R. E. Moeller. 2015. Ecological consequences of long-term browning in lakes. Sci. Rep. **5**: 18666. doi:10.1038/srep18666

Xiao, Y., T. Sara-Aho, H. Hartikainen, and A. V. Vähätalo. 2013. Contribution of ferric iron to light absorption by chromophoric dissolved organic matter. Limnol. Oceanogr. **58**: 653–662. doi:10.4319/lo.2013.58.2.0653

Xiao, Z., S. Liang, R. Sun, J. Wang, and B. Jiang. 2015. Estimating the fraction of absorbed photosynthetically active radiation from the MODIS data based GLASS leaf area index product. Remote Sens. Environ. **171**: 105–117. doi:10.1016/j.rse.2015.10.016

Yang, X., C. M. O'Reilly, J. R. Gardner, M. R. V. Ross, S. N. Topp, J. Wang, and T. M. Pavelsky. 2022. The color of Earth's lakes. Geophys. Res. Lett. **49**: e2022GL098925. doi:10.1029/2022GL098925

Ylöstalo, P., K. Kallio, and J. Seppälä. 2014. Absorption properties of in-water constituents and their variation among various lake types in the boreal region. Remote Sens. Environ. **148**: 190–205. doi:10.1016/j.rse.2014.03.023

Acknowledgments

We thank everyone involved in data collection and laboratory work within the projects connected to this study. The University of Jyväskylä provided a graduate fund to SAA. Academy of Finland provided funding to RIJ, HH, MT, and KMV (research grant numbers 285619 (ALLOCARB), 260797 (RNA-unit), and 311229 (MiDAS)). The RNA-unit and the ALLOCARB projects supplied the samples from part of the 128 lakes in the primary dataset.

Conflict of Interest

None declared.

Submitted 22 June 2023
Revised 28 September 2023
Accepted 21 December 2023

Associate editor: Yunlin Zhang